

Organization of strongly interacting directed polymer liquids in the presence of strong constraints

Anton Souslov,¹ D. Zeb Rocklin,² and Paul M. Goldbart¹

¹*School of Physics, Georgia Institute of Technology, Atlanta, GA 30332, USA*

²*Department of Physics, University of Illinois at Urbana-Champaign,
1110 West Green Street, Urbana, IL 61801, USA*

(Dated: December 3, 2024)

The impact of impenetrable obstacles on the energetics and equilibrium structure of strongly repulsive directed polymers is investigated. As a result of the strong interactions, regions of severe polymer depletion and excess are found in the vicinity of the obstacle, and the associated free-energy cost is found to scale quadratically with the average polymer density. The polymer-polymer interactions are accounted for via a sequence of transformations: from the 3D line liquid to a 2D fluid of Bose particles to a 2D composite fermion fluid and, finally, to a 2D one-component plasma. The results presented here are applicable to a range of systems consisting of noncrossing directed lines.

PACS numbers: 36.20.Ey, 71.10.Pm, 05.30.Jp, 52.27.Aj

Many investigations of $(d+1)$ -dimensional systems of directed lines hinge on an analogy between the statistical mechanics of these systems and the quantum mechanics of d -dimensional systems of nonrelativistic bosonic particles [1]. This analogy has proven useful in work on directed line liquids, such as those consisting of directed polymers (either under tension [2] or within a nematic solvent [3]) as well as fluctuating line defects in symmetry-broken phases, such as vortex lines in type-II superconductors [4].

In this Letter, we focus on the specific example of a liquid of many thin thermally fluctuating polymers under tension, which interact with one another via a strong short-range repulsion. We represent this liquid in terms of $(2+1)$ -dimensional directed lines, and we treat the polymer repulsion as a restriction on the possible configurations, prohibiting the intersection of any two lines. Central to the present work is the non-perturbative treatment of this nonintersection restriction, which we accomplish via the well-known Chern-Simons transmutation of quantum statistics, from Bose to Fermi. Using quantum many-body theory, we address two fundamental questions regarding this system, viz., “What are the free-energy cost and equilibrium polymer density induced by an impenetrable inclusion, i.e., a region in which the polymer density is forced to be zero?” We note that the free-energy cost of the inclusion corresponds to the probability that the unconstrained system would spontaneously satisfy the constraint. For simplicity, we study thin, flat inclusions within a planar slice perpendicular to the polymer direction \hat{z} , and we determine the equilibrium polymer density within that slice. More generally, we determine the free energy and equilibrium density in the presence of spatially extended constraints, such as a ring, positioned in the slice, threaded by a fixed number of polymers, as shown in Fig. 1. The inclusion is precisely the case for which no polymers thread the ring.

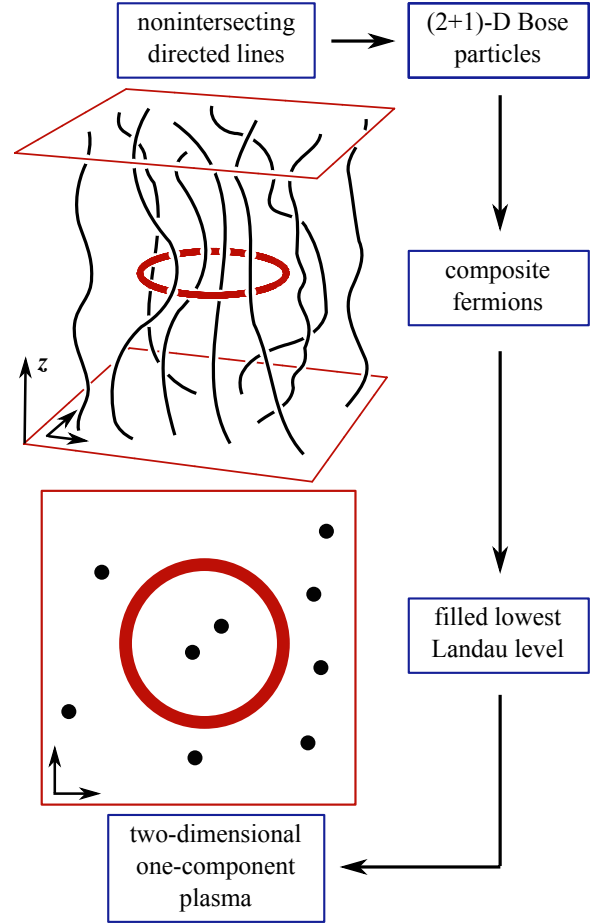


FIG. 1. (Color online) Sequence of transformations of a liquid of directed polymers subject to a spatially extended constraint, shown as a ring (thick line), threaded by a fixed number of polymers. The sequence is used to obtain the free energy and polymer density of the constrained system. Ultimately, the directed polymer liquid is transformed to a two-dimensional one-component plasma, whose the Coulomb repulsion results from integrating out the long noncrossing chains.

We emphasize that the dominant free-energy cost of such constraints is the result of the many-body effect of the crowding of the polymers, an effect absent for free directed lines.

The transformation between directed lines and bosons enables one to harness powerful techniques from quantum many-body physics for application to directed line liquids. The first such application was due to de Gennes, who invoked it to calculate the structure factor for a (1+1)-dimensional hard-core directed line liquid [2]. A recent elaboration on these results by Rocklin *et al.* yielded the free energy and equilibrium polymer density in the presence of pins and other impenetrable constraints for the same system [5]. In essence, de Gennes's strategy separates into two major steps. First, the classical (1+1)-dimensional noncrossing directed lines are mapped into quantum hard-core point bosons moving in one dimension [1]. Second, these hard-core bosons are mapped, exactly, to free fermions [6]. The virtue of this sequence of transformations, which we are here seeking to emulate for (2+1)-dimensional systems of noncrossing directed lines, is that it reduces the strongly interacting directed line liquid to an (exactly solvable) system of free fermions. We accomplish a similar reduction by mapping our (2+1)-dimensional directed line liquid to a two-dimensional fluid of Bose particles, and then make the Chern-Simons transmutation from Bose to Fermi statistics [7].

We address a model of the line liquid that consists of N paths that are directed along the z -axis from $z = 0$ to $z = L$ via a line tension τ , which penalizes deflections of the paths. We assume no path switchbacks, in which case the (Cartesian) (x, y) -coordinates of the N paths $\mathbf{R}(z) \equiv \{\mathbf{r}_n(z)\}_{n=1}^N$ are single-valued functions of z . We study interactions that are short-ranged and so strong that they prohibit configurations in which any pair (n, n') of lines intersect, i.e., in which $\mathbf{r}_n(z) = \mathbf{r}_{n'}(z)$ for any value of z . The statistical weight for noncrossing configurations is then proportional to $\exp(-\mathcal{G}/T)$, where

$$\mathcal{G} \equiv \frac{\tau}{2} \sum_{n=1}^N \int_0^L dz \left| \frac{d\mathbf{r}_n}{dz} \right|^2, \quad (1)$$

and the temperature T is measured in units of the Boltzmann constant. Correspondingly, the partition function Z is given by the functional integral $Z = \int [D\mathbf{R}(\cdot)] e^{-\mathcal{G}/T}$, taken over all noncrossing paths [8].

To implement the mapping to quantum many-body physics we note that $Z = \langle \Psi^F | e^{-\beta L \mathcal{H}} | \Psi^I \rangle$; see, e.g., Ref. [1]. The quantum Hamiltonian,

$$\mathcal{H} = \frac{1}{2m} \sum_{n=1}^N |\mathbf{p}_n|^2, \quad (2)$$

describes two-dimensional Bose particles of mass m under the correspondence $(\tau, T) \leftrightarrow (m, \hbar)$. In addition, the

quantum amplitudes $\langle \mathbf{R} | \Psi^{I/F} \rangle$ reflect the initial and final *a priori* classical end-point distributions. The quantum states $|\mathbf{R}\rangle$ are symmetrized products of N single-particle position eigenstates $|\mathbf{r}\rangle$, appropriate for indistinguishable polymers. Observe that the limit $L \rightarrow \infty$ is also the low-temperature limit $\beta \rightarrow \infty$, for which the quantum ground state dominates Z .

Our focus is on the increase of the free-energy $\Delta\mathcal{F}$ ($\equiv \mathcal{F}_c - \mathcal{F}_u$) from \mathcal{F}_u (its value in the *unconstrained* directed line liquid) to \mathcal{F}_c (its value in the liquid with a spatially extended *constraint*). We compute $\Delta\mathcal{F}$ using the ratio between the unconstrained partition function Z and the partition function Z_c , which includes the effects of constraint. If, as in the case we consider, the constraint requires that exactly Q directed lines pass through some two-dimensional region \mathcal{D} perpendicular to the director $\hat{\mathbf{z}}$ and far from the ends $z = 0, L$, then, in the limit $L \rightarrow \infty$, $\Delta\mathcal{F}$ may be computed using ground-state dominance as:

$$\Delta\mathcal{F} = -T \ln \frac{Z_c}{Z} = -T \ln \int_{\mathcal{C}} d\mathbf{R} |\Psi_b(\mathbf{R})|^2. \quad (3)$$

Here, \mathcal{C} indicates the constraint on integration that exactly Q of the N coordinates $\{\mathbf{r}_n\}$ lie within \mathcal{D} . The ground-state wavefunction in Eq. (3) $\Psi_b(\mathbf{R})$ ($\equiv \langle \mathbf{R} | \text{GS} \rangle$) is the lowest-energy (particle-exchange symmetric) solution of the energy eigenproblem $\mathcal{H}\Psi_b = E\Psi_b$. Thus, we are confronted with the task of finding an expression for $|\Psi_b|^2$.

The restrictions $\mathbf{r}_n(z) \neq \mathbf{r}_{n'}(z)$ on the path integrals for the line-liquid partition functions Z and Z_c demand a nonperturbative treatment. Following the essence of de Gennes's [2] strategy, we transmute the statistics of the quantum fluid from Bose to Fermi [7], thus arriving at a description in terms of a many-fermion wavefunction Ψ_f that necessarily has nodes for any two coincident particles, i.e., $\Psi_f(\mathbf{r}_1, \dots, \mathbf{r}, \dots, \mathbf{r}, \dots, \mathbf{r}_N) = 0$. This transmutation is accomplished via the well-known [9] singular gauge transformation of Chern-Simons theory: $\Psi_b \rightarrow \Psi_f \equiv \Psi_b \exp(i\phi \sum_{n' < n} \theta_{n,n'})$, where $\theta_{n,n'} \equiv \tan^{-1}[(y_n - y_{n'})/(x_n - x_{n'})]$ is the polar angle between particles n and n' . Then, under the exchange of particles n and n' , $\theta_{n,n'} \rightarrow \theta_{n,n'} \pm \pi$, and, provided ϕ is an odd integer, Ψ_f is antisymmetric, i.e., fermionic. As Ψ_b is the ground state of \mathcal{H} , Eq. (2), Ψ_f obeys the transmuted energy eigenproblem [9] $\mathcal{H}'\Psi_f = E'\Psi_f$, where

$$\mathcal{H}' \equiv \frac{1}{2m} \sum_{n=1}^N |\mathbf{p}_n - q\mathbf{A}_n(\mathbf{r}_n)|^2, \quad (4a)$$

$$\mathbf{A}_n(\mathbf{r}) \equiv \frac{\phi\hbar}{2\pi q} \sum_{n'(\neq n)} \nabla'_n \theta_{n,n'} = \frac{\phi\hbar}{2\pi q} \sum_{n'(\neq n)} \frac{\hat{\mathbf{z}} \times (\mathbf{r} - \mathbf{r}_{n'})}{|\mathbf{r} - \mathbf{r}_{n'}|^2}. \quad (4b)$$

\mathcal{H}' has the same energy spectrum as \mathcal{H} , so for any eigenstate, including the ground state, $E' = E$.

If, in Eq. (4a), $\mathbf{A}_n(\mathbf{r}_n)$ were to depend only on \mathbf{r}_n and not on any $\{\mathbf{r}_{n'(\neq n)}\}$, the Hamiltonian \mathcal{H}' would describe independent particles in a magnetic field $\nabla \times \mathbf{A}$. However, as shown in Eq. (4b), \mathbf{A}_n does depend on $\{\mathbf{r}_{n'(\neq n)}\}$, which implies (nonlocal) interactions between all particles. Equation (4b) states that $\{\mathbf{A}_n\}$ describes particles that have ϕ quanta of fictitious magnetic flux attached (i.e., localized at the position of every particle, each quantum carrying h/q flux, where q is a fictitious charge). Thus, \mathcal{H}' describes composite fermions—composed of particles obeying Fermi statistics and flux tubes [10, 11]. This transmutation of statistics is the Hamiltonian form of Chern-Simons theory [12].

Although this formulation effectively incorporates the hard-core restriction, it remains intractable, and thus we are led to take advantage of a natural approximation (see, e.g., Refs. [10, 11]), which we now describe. Instead of having an odd number of flux tubes attached to each particle, we smear the magnetic field associated with one flux tube per particle uniformly over the area of the system, and gauge-transform away the remaining flux tubes. In this so-called Average Field Approximation (AFA), the fermions are *non-interacting* and subject to a *homogeneous* magnetic field $\nabla \times \mathbf{A} = B\hat{\mathbf{z}}$, corresponding to one quantum of magnetic flux per particle. [In the symmetric gauge, $\mathbf{A} = B(y, -x, 0)/2$.] In the language of directed lines, the magnetic field is equal to the number of lines per unit area ρ_0 times a quantum of flux (i.e., $B = \rho_0 h/q$). In this magnetic field, the many-body ground-state has energy $E = NB\hbar q/2m$ and the wave-function Slater determinant takes the Vandermonde form [13]

$$\Psi_f^a(\mathbf{R}) \propto e^{-\sum_{n=1}^N |w_n|^2/4\ell^2} \prod_{1 \leq n < n' \leq N} (w_n - w_{n'}), \quad (5)$$

where $w_n \equiv x_n + iy_n$. Within this approximation, the quantum ground-state energy and wave-function describe a long, noncrossing, directed line liquid. In particular, for its free energy per unit volume $g (\equiv \langle \mathcal{G} \rangle / AL)$, we obtain the result

$$g = \pi T^2 \rho_0^2 / \tau. \quad (6)$$

As Eq. (5) gives an expression for the ground-state wave-function, we proceed with our goal of calculating the increase in the free energy $\Delta\mathcal{F}$ by using the integral in Eq. (3). We thus make the approximation $|\Psi_b|^2 \approx |\Psi_f^a|^2$, and compute $\Delta\mathcal{F} = -T \ln \int_{\mathcal{D}} d\mathbf{X} \exp(-U(\mathbf{R})/T)$, where

$$-\frac{U(\mathbf{R})}{T} \approx \ln |\Psi_f^a|^2 = 2 \sum_{1 \leq n < n' \leq N} \ln |\mathbf{r}_n - \mathbf{r}_{n'}| - \pi \rho_0 \sum_{n=1}^N |\mathbf{r}_n|^2. \quad (7)$$

Interpreted as a potential energy, U describes a two-dimensional one-component plasma (2DOCP) [18, 19]. In the general case of the plasma, particles of (e.g.,

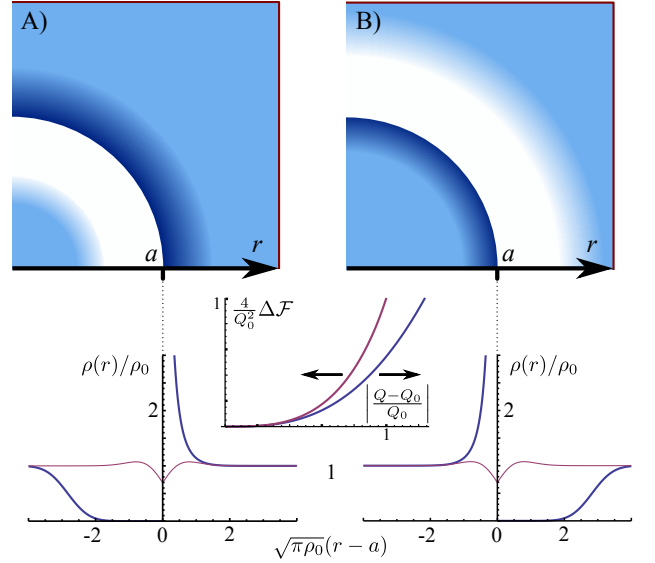


FIG. 2. (Color online) Two-dimensional one-component plasma (2DOCP) subject to a spatially extended constraint. The electrostatic approximation predicts a gap in the mobile charge density and an accumulated surface charge for cases (A), for which the excess mobile charge resides outside the ring, and (B), for which the excess mobile charge is confined inside the ring. This approximation also predicts discontinuities in the mobile-charge density, which in the exact solution are smeared out due to thermal fluctuations of the mobile charges around the minimum energy state. The exact solution leads to the density profiles $\rho(r)/\rho_0$ shown for $(Q - Q_0)/\sqrt{2Q_0} = \pm 4$ (thick) and 0 (thin), where $-Q$ and $Q_0 (\equiv \pi a^2 \rho_0)$ are the mobile and background charges inside the ring, respectively [14, 15]. The inset shows the rescaled energy cost $(4/Q_0^2) \Delta\mathcal{F}$ [top: case (A), bottom: case (B)] [16]. The curves are valid for macroscopic values of the charge deficiency, i.e., for not-too-small values of the argument, when $\Delta\mathcal{F}$ is dominated by electrostatic energy. In the text, we establish that these profiles corresponds to the in-plane distribution of noncrossing directed lines due to a planar spatially extended constraint.

negative) charge $-e$ inhabit a uniform background that maintains overall charge neutrality, and they interact via the two-dimensional Coulomb repulsion: $e^2 \ln |\mathbf{r}_n - \mathbf{r}_{n'}|$. This U/T corresponds to a specific value, viz. 2, of the plasma coupling constant e^2/T . Applied to the plasma, the measure $\int_{\mathcal{D}} d\mathbf{R}$ in $\Delta\mathcal{F}$ requires exactly Q mobile charges to occupy the region of constraint \mathcal{D} .

This completes our reduction of the three-dimensional classical liquid of noncrossing directed lines to the classical two-dimensional one-component plasma (2DOCP); this reduction enables us to compute physical properties such as the free-energy cost and the equilibrium density profiles associated with the imposition of spatially extended constraints. The long-range planar interactions within the 2DOCP arise from the short-range interactions between the fluctuating directed lines, integrated over their length. To calculate the free energy and the

equilibrium density of the directed line liquid in the presence of a ring constraint, we analyze the 2DOCP, first at the level of classical electrostatics, and then allowing for fluctuations. Note that the constraint results in regions of excess mobile charge and regions partially depleted of mobile charge. To minimize the electrostatic energy, any excess mobile charge is forced up against the boundary of \mathcal{D} . Moreover, on the other side of the boundary, a region fully depleted of mobile charge (i.e., a gap) opens up, out to a radius within which the net charge is zero [17].

Similarly, at the level of electrostatic energy minimization one can readily determine the energy of the charge distribution and, hence, the free-energy cost of the constraint $\Delta\mathcal{F}(Q, Q_0)$, in terms of the mobile charge $-Q$ and the background charge within \mathcal{D} , i.e., $Q_0 (\equiv \pi a^2 \rho_0)$, both in units of e [16]; see Fig. 2. For the special case $Q = 0$ (i.e., \mathcal{D} empty, corresponding to an inclusion) the free-energy cost has a simple form: $\Delta\mathcal{F} = Q_0^2/4 = \pi^2 a^4 \rho_0^2/4$. This electrostatic result is significant for the noncrossing-directed-line liquid, as it differs qualitatively from the case of a noninteracting directed line liquid, for which a particle inclusion incurs a free-energy cost *linear* in $a^2 \rho_0$.

To improve upon the electrostatic approximation, we take into account the effect of thermal fluctuations on the polymer density profile. We rely on the exact solution of the 2DOCP with the appropriate plasma coupling constant, i.e., 2; see Refs. [14–16, 19, 20]. In the limit $a \gg 1/\sqrt{\rho_0}$, the exact density profile outside the region of constraint depends only on a , ρ and Q through the combination $(Q - Q_0)/\sqrt{2Q_0}$ [14]. The layer of excess mobile charge on one side forms an electrical double layer of thickness of order $1/\sqrt{\rho_0}$; see Fig. 2c and Ref. [14]. The region partially depleted of mobile charge does develop a soft gap, in which the charge is small but nonzero. The mobile charge density profile progresses smoothly, according to a qualitatively error-function-like curve, through the boundary region, rapidly approaching the value that exactly compensates the background charge density ρ_0 ; see Fig. 2c and Ref. [14]. The mobile charge density profile for the depleted side of the constraint applies to both cases, $Q > Q_0$ and $Q < Q_0$, and similarly for the excess-charge side. For Q small relative to Q_0 , the remaining mobile charge in \mathcal{D} forms a droplet whose shape is essentially the density profile of a system of electrons that fill the lowest Landau level: a flat central profile and a decay into the soft gap; see, e.g., Ref. [21]. Thus, we have established that when some fixed portion of the lines of a directed line liquid is constrained to thread \mathcal{D} , the equilibrium density profile in the slice containing \mathcal{D} is that of the correspondingly constrained 2DOCP.

Recapping our strategy, we progressed from a three-dimensional liquid of thermally fluctuating lines, to a two-dimensional quantum many-boson fluid, to a two-

dimensional quantum many-fermion fluid coupled to a Chern-Simons gauge field, which we treated in the Average Field Approximation to obtain the filled lowest Landau level picture. The phenomenology of a lowest Landau level filled with noninteracting fermions is well studied, and suggests various analogous phenomena for the corresponding hard-core boson fluid. However, as the AFA is an approximation, these analogous phenomena may be artifacts of the approximation, and we now use physical intuition to identify any such artifacts. For example, the quantum Hall effect suggested by the AFA is one such artifact: the boson fluid does not have broken time-reversal symmetry, and therefore shows no Hall effect [25–27]. A second artifact is suggested by the incompressibility of the filled lowest Landau level, which would incorrectly imply the incompressibility of the boson fluid. However, by reinstating the inter-particle interactions $\mathbf{A}(\mathbf{r}) - \mathbf{A}_a(\mathbf{r})$, e.g., via the Random Phase Approximation, the compressibility of the boson fluid is restored, as shown in Refs. [25, 26]. In the context of the directed line liquid, the thermodynamic (areal) compressibility κ is defined in terms of the free energy density g via $\kappa^{-1} \equiv \rho_0^2 \partial^2 g / \partial \rho_0^2$, and thus, using Eq. (6), we obtain $\kappa = \tau / 2\pi T^2 \rho_0^2$. A particularly noteworthy consequence of the residual interactions $\mathbf{A}(\mathbf{r}) - \mathbf{A}_a(\mathbf{r})$ is their ability to renormalize the effective plasma coupling constant e^2/T in the plasma analogy away from the exactly solvable case, viz., 2. Nevertheless, we expect the general picture presented here, of the energetics and structure of the directed line liquid in the presence of spatially extended constraints, to hold.

Motivation for this work arose through discussions with Jennifer Curtis, which we gratefully acknowledge. One of us (PMG) thanks for its hospitality the Aspen Center for Physics, where some of this work was undertaken. This work was supported in part by NSF DMR 09 06780 and DMR 12 07026.

-
- [1] R. P. Feynman, *Statistical Mechanics: A Set of Lectures* (Basic Books, 1972).
 - [2] P. G. de Gennes, J. Chem. Phys. **48**, 2257 (1968).
 - [3] R. D. Kamien, P. Le Doussal, and D. R. Nelson, Phys. Rev. A **45**, 8727 (1992).
 - [4] D. R. Nelson and H. S. Seung, Phys. Rev. B **39**, 9153 (1989).
 - [5] D. Z. Rocklin, S. Tan, and P. M. Goldbart, Phys. Rev. B **86**, 165421 (2012).
 - [6] M. Girardeau, J. Math. Phys. **1**, 516 (1960).
 - [7] A. M. Polyakov, Mod. Phys. Lett. A **03**, 325 (1988).
 - [8] To fully specify the partition function we impose permutation-symmetric *a priori* probability distributions on $\mathbf{R}(0)$ and independently on $\mathbf{R}(L)$. This enables us to exploit bosonic quantum states.
 - [9] D. P. Arovas, J. R. Schrieffer, F. Wilczek, and A. Zee, Nucl. Phys. B **251**, 117 (1985).

- [10] F. Wilczek, *Fractional Statistics and Anyon Superconductivity* (World Scientific, 1990).
- [11] J. Jain, *Composite Fermions* (Cambridge University Press, 2007).
- [12] This composite fermion theory has been used in many contexts, including discussions of the fractional quantum Hall effect [10, 11], anyon superconductivity [10], and reptation dynamics in polymer melts [28]. The topological nature of Chern-Simons field theory has been used to study the winding [29], writhe [30] and knot invariants [31] of entangled polymers. The Lagrangian form of Chern-Simons theory involves coupling the Bose particles to a gauge field and integrating out the gauge field to find an effective fermion theory [9, 22–24].
- [13] R. B. Laughlin, Phys. Rev. B **27**, 3383 (1983).
- [14] B. Jancovici, J. Phys. Lett. **42**, 223 (1981).
- [15] B. Jancovici, J. Stat. Phys. **28**, 43 (1982).
- [16] B. Jancovici, J. L. Lebowitz, and G. Manificat, J. Stat. Phys. **72**, 773 (1993).
- [17] For an arbitrary, simply-connected, compact region \mathcal{D} , the charge-density profile that minimizes the electrostatic energy may be addressed using a conformal mapping from this circular geometry.
- [18] R. B. Laughlin, Phys. Rev. Lett. **50**, 1395 (1983).
- [19] B. Jancovici, Phys. Rev. Lett. **46**, 386 (1981).
- [20] B. Jancovici, J. Stat. Phys. **29**, 263 (1982).
B. Jancovici, J. Stat. Phys. **34**, 803 (1984).
- [21] X. Wen, *Quantum Field Theory of Many-Body Systems* (Oxford University Press, 2004).
- [22] N. Read, Phys. Rev. Lett. **62**, 86 (1989).
- [23] S. C. Zhang, T. H. Hansson, and S. Kivelson, Phys. Rev. Lett. **62**, 82 (1989).
- [24] A. Lopez and E. Fradkin, Phys. Rev. B **44**, 5246 (1991).
- [25] A. L. Fetter, C. B. Hanna, and R. B. Laughlin, Phys. Rev. B **39**, 9679 (1989).
- [26] Q. Dai, J. L. Levy, A. L. Fetter, C. B. Hanna, and R. B. Laughlin, Phys. Rev. B **46**, 5642 (1992).
- [27] By Hall effect we mean the occurrence of a transverse particle current in response to a longitudinal potential gradient.
- [28] A. L. Kholodenko and T. A. Vilgis, J. Phys. I France **4**, 843 (1994).
- [29] B. Drossel and M. Kardar, Phys. Rev. E **53**, 5861 (1996).
- [30] J. D. Moroz and R. D. Kamien, Nucl. Phys. B **506**, 695 (1997).
- [31] F. Ferrari and I. Lazzizzera, Nucl. Phys. B **559**, 673 (1999).